# Effects of coupling disorder on the phase dynamics of superconducting clusters

S. V. Rao and D. J. Van Harlingen
*Department of Physics, University of Illinois at Urbana-Champaign, 1110 West Green Street, Urbana, Illinois 61801*
(Received 18 June 1993)

We have studied the electrical transport properties of superconducting clusters, periodic arrays of Josephson-coupled superconducting islands containing only a few cells. In such small samples, variations in the coupling between adjacent islands are not averaged out and produce asymmetries in the magnetoresistance as a function of bias current and applied magnetic field. By comparing experimental results with computer simulations of the Josephson phase dynamics in the clusters, we are able to understand the origin of the observed asymmetries and obtain a quantitative estimate of the coupling disorder in our arrays.

Arrays of weakly coupled superconductor islands have been extensively used as model systems for studying fundamental problems in condensed-matter physics, including two-dimensional phase transitions, phase coherence, frustration, and vortex dynamics.[1] The primary advantage of arrays is the ability to control the geometry, coupling, and material properties by photolithographic patterning and thin-film microfabrication. Normally, large arrays containing $10^4-10^6$ islands are used for these studies in order to minimize the effects of the edges and to enhance signal levels. In large arrays, disorder in the cell areas and intergrain coupling is averaged out, generally resulting only in a smearing of structure in the magnetoresistance. In particular, studies have been made in which random cell area disorder,[2] discrete vortex pinning defects,[3] and percolative site disorder[4] have been deliberately and controllably introduced into periodic arrays. It is not possible in these large arrays, however, to extract information about the microscopic distributions and dynamics of vortices, or to resolve the effect of individual defects.

Our approach is to study arrays in which the number of islands (and cells) is rather small, typically less than $5\times5$. We refer to such arrays as clusters. A superconducting cluster is a mesoscopic system—large enough to exhibit the long-range phase coherence and vortex interactions present in large arrays, but small enough that disorder and discrete vortex motion are not averaged out. Clusters have the added advantage that they are small enough that we can perform computer simulations of the Josephson phase dynamics and compare them directly to measurements that probe vortex motion. Such microscopic simulations are not possible in large arrays, and the gap between static thermodynamic properties accessible by theory and the experimental dynamical measurements has long been an impediment to the study of weakly coupled arrays of networks of superconducting lines. In this paper, we present measurements of the magnetoresistance of $2\times2$ clusters and corresponding computer simulations. This enables us to understand the origin of observed asymmetries and obtain a quantitative estimate of the coupling disorder in our arrays.

Figure 1 shows an electron micrograph of a $2\times2$ cluster in which superconducting Pb islands are coupled by Pb-Cu-Pb SNS (superconductor-normal-superconductor) proximity-effect junctions. These samples are fabricated by a two-step process. First, using a liftoff process we pattern a square grid of lines consisting of 120 nm of Pb on top of 180 nm of Cu, deposited sequentially. The linewidth is 2 $\mu$m; the cell size is 20 $\mu$m$\times$20 $\mu$m. Second, we form a junction in the center of each line segment by etching away the Pb using Ar-ion milling to create a tunneling gap of about 1.3 $\mu$m between adjacent islands. We have also fabricated Nb-Al-Nb clusters using reactive ion etching to define the junctions. The islands

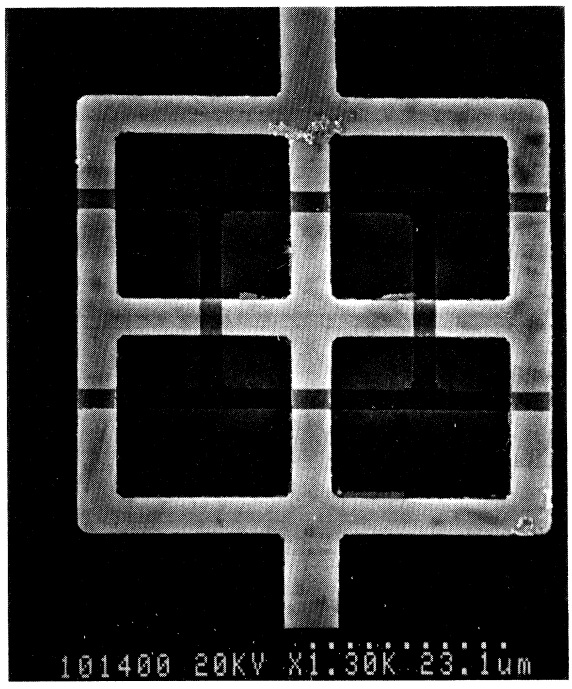


FIG. 1. Scanning electron micrograph of a Pb-Cu-Pb $2\times2$ cluster array. The cell size is 20 $\mu$m $\times$20 $\mu$m; the gap between islands is typically 1.3 $\mu$m.

 

at each end are shorted together by superconducting electrodes through which current can be injected and extracted. The voltage across the clusters as a function of temperature, applied perpendicular magnetic field, and bias current is measured using a rf-superconducting quantum interference device (SQUID) in a potentiometric circuit with a voltage sensitivity of 100 pV. Measurements are made in a $He^4$ cryostat placed in a rf-shielded room; the sample and SQUID circuitry are magnetically shielded using a superconducting Pb can and a double mu metal shield that reduces the ambient magnetic field to about 1 mG. A Helmholtz coil is used to apply a uniform magnetic field perpendicular to the array.

In order to compare our measurements of the cluster voltages, we have carried out computer simulations of the phase dynamics of cluster arrays. Details of the simulations will be presented elsewhere.[5] The gauge-invariant phase difference across each junction is evolved in time according to the resistively-shunted-junction (RSJ) model, constrained by phase coherence around each cell, until a stable static phase configuration (zero-voltage state) is reached, or until a steady dynamical state with a finite time-averaged voltage is established. The static vortex configurations and dynamical modes depend on the magnetic field through the frustration parameter $f=\Phi/\Phi_0$, the applied flux per cell. In Fig. 2(a), we show the calculated voltage versus applied flux per cell for a perfect $2\times2$ cluster with uniform coupling. Curves for positive and negative flux and both current directions are shown. As expected, the voltage has even symmetry with respect to magnetic-field direction and odd symmetry with respect to current polarity. The array voltage exhibits a flux periodicity of $1\Phi_0$ per cell, with substructure at $f=\frac{1}{4}$, $\frac{1}{2}$, and $\frac{3}{4}$, and is symmetric about $f=\frac{1}{2}$. This symmetry arises because the zero vortex state at $f=0$ and the state with one vortex per cell at $f=1$ are equivalent. A dynamical vortex state at flux $f$ is, therefore, equivalent to the motion of antivortices (vortices of opposite polarity) at flux $(1-f)$.

The voltage versus flux response of real clusters is not as simple. In Fig. 2(b), we show measurements of the voltage versus flux for a $2\times2$ cluster for both polarities of flux and current. The most obvious feature of the data is the asymmetry with respect to flux. Although the voltage is still periodic in applied flux, the mirror symmetries about $f=0$, $I=0$, and $f=\frac{1}{2}$ are not present. Relative to the perfect array, some features are enhanced and others suppressed. We attribute the asymmetry to disorder in the critical currents coupling the islands in the cluster. The critical current depends both on the geometry and on the normal-state conductance of the SNS junctions. The most sensitive parameter is the tunneling gap which affects the critical current density exponentially. We have modeled the observed voltage-flux curves by introducing junction coupling disorder into the simulations of the vortex dynamics. As shown in Fig. 2(c), we obtain reasonable agreement with the data by assuming that several of the junctions have substantially (up to a factor of 2) different critical currents from the rest. Although the fit is not exact, the relative size and location of the principal features in the data are reproduced. Further, the dependence on the polarities of the field and current are accurately predicted. Another computer simulation fit to data from a Nb-Al-Nb sample is shown in Fig. 3,

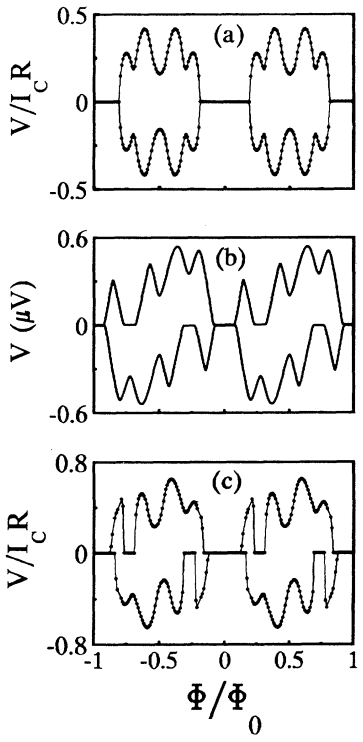


FIG. 2. Voltage vs applied magnetic flux per cell for $2\times2$ clusters for positive and negative bias currents. (a) Dynamical simulation for a perfect $2\times2$ cluster, (b) measurements for a microfabricated $2\times2$ proximity-coupled cluster at a temperature of 1.3 K, (c) simulation incorporating coupling disorder modeled to fit the data in (b).

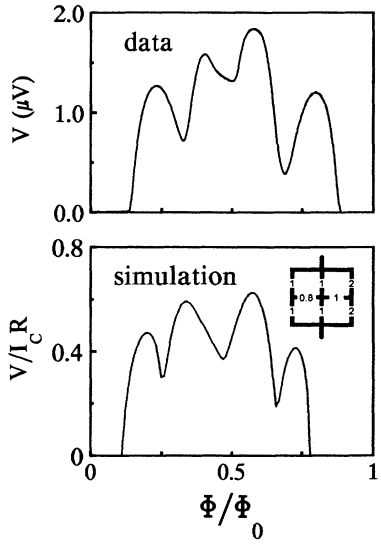


FIG. 3. Voltage vs applied flux data taken for a Nb-Al-Nb $2\times2$ cluster compared to a computer simulation of the disordered array shown.

along with the configuration of critical currents used in the modeling.

The required variation in the critical currents for the junctions (of order 50–100%) is typical for clusters we have fabricated and modeled. The critical current of a SNS junction varies as $\exp(-d/\xi_n)$, where $d$ is the width of the proximity gap and $\xi_n=(h v_F l/6k_B T)^{1/2}$ is the normal-state coherence length that depends on the mean-free-path $l$ and the Fermi velocity $v_F$ of the normal metal.[6] Scanning electron microscopy indicates a proximity gap of $1.3\pm0.2$ $\mu$m, within the expected resolution for optical lithography. For our junctions, assuming a mean-free-path $l$ limited by boundary scattering, we estimate $\xi_n$ to be about 0.4 $\mu$m at the coupling temperature of 2 K. Thus, lithographic variations in the gap width $\Delta d$ should modify the critical current by $\Delta d/\xi_n \sim 50\%$, in reasonable agreement with our measurements. Since we use the same fabrication techniques for our larger arrays, we expect the variation in critical currents to be comparable in those systems. However, due to averaging, the voltage versus flux curves are always found to be nearly symmetric and lack sharp features.

Although the disorder introduces asymmetry into the voltage versus flux response, two inversion symmetries are apparent in both the data and the simulations. There is inversion symmetry through the origin ($f=0, I=0$) and through the point ($f=\frac{1}{2}, I=0$). The inversion through the origin is required by time-reversal symmetry—reversing both the field and current yields a distribution of total current (bias plus circulating) time reversed from the original current pattern. The inversion symmetry about the $f=\frac{1}{2}$ point is more subtle and depends on the dynamics of vortices and antivortices in the disordered cluster. First, we examine the energy of the static vortex configurations versus flux with and without bias current, shown in Fig. 4 for the perfect $2\times2$ cluster and for the disordered array modeled in Fig. 3. The energy scale is given in units of the Josephson coupling energy $E_J=I_0\Phi_0/2\pi$, where $I_0$ is the average critical current of the junctions. In all cases, as the field is increased from $f=0$ to $f=1$, the number of vortices in the lowest-energy state steps from 0 to 4. Without bias current, the degeneracy of vortex configurations consisting of one, two, or three vortices is broken by disorder, but the mirror symmetry about $f=\frac{1}{2}$ remains. Current flow in the perfect array also causes a symmetric splitting of the energy levels. However, when bias current is applied to a disordered cluster, the energy becomes asymmetric about $f=\frac{1}{2}$ due to the interaction of the bias current with the distorted circulating currents. Alternately, we can understand the asymmetry as a consequence of disorder breaking the symmetry of vortices and antivortices in the array in the presence of a current.

Although a multidimensional washboard phase potential is the most complete description of the cluster system, it is more physical to think in terms of spatial vortex motion across the cluster. We can model the diffusion of an isolated vortex in the cluster as a particle moving in a modulated potential. This picture has been discussed by Rzchowski *et al.*[7] for perfect infinite square arrays in which the vortex sees a uniform two-dimensional periodic potential. In a finite-size cluster, the potential is strongly modified by edge effects. Vortex entry and exit barriers on the edges are enhanced by screening currents in the array, as has been previously discussed for ladder samples.[8] Coupling disorder further distorts the vortex potential, making each energy barrier different for a vortex crossing the array. As noted above, the array simulations can determine the energy of any stable vortex

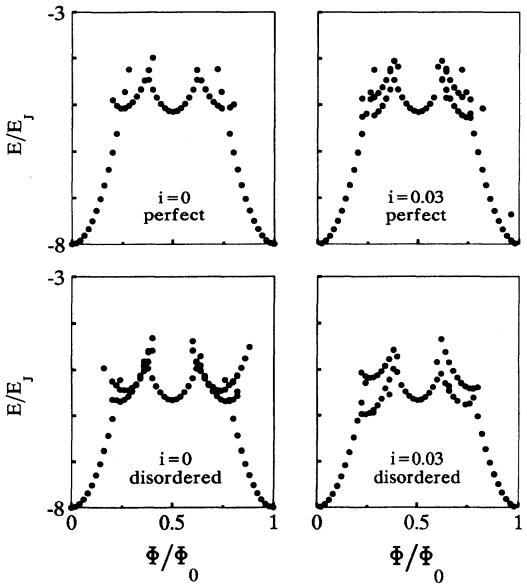


FIG. 4. Calculated Josephson coupling energy vs applied magnetic field for a perfect $2\times2$ cluster and for the disordered array of Fig. 3 at zero current and for a finite current bias $I=0.03I_0$.

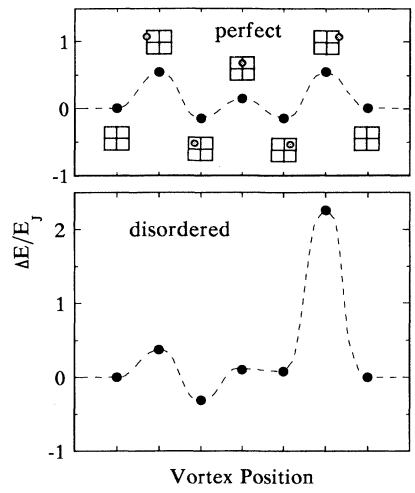


FIG. 5. Spatial variation of the energy potential at magnetic flux $f=\frac{1}{4}$ for a single vortex in a perfect $2\times2$ cluster and the disordered cluster of Fig. 3. The energy scale is relative to the array energy in the absence of a vortex. Application of a bias current effectively tilts the modulated potential, allowing vortex motion.

configuration at any applied field and bias current and for any distribution of junction critical currents. To calculate the barriers for vortex motion, we force the vortex to sit at the location of the junction between two cells or at the edge of the cluster by forcing the junction phase to $\pi$ and calculating the cluster energy. This gives the energy of the saddle point separating two stable vortex positions. Potential curves for the perfect and disordered $2\times2$ clusters discussed above are shown in Fig. 5, calculated for $f=\frac{1}{4}$, for which the energy of the zero and one vortex states in the perfect cluster are about equal. The energy is plotted relative to the state with no vortices. We emphasize that only the extrema can be specifically calculated, the dashed curve is drawn as a guide to the shape of the potential but has no physical significance.

For the perfect array, the potential is symmetric about the center. The barrier between the cells is about $\frac{1}{5}$ of the height of the edge barriers. The effect of a bias current can be roughly viewed as a tilting of the spatial potential—as the magnitude of the current is increased in either polarity, the entry barrier drops until modulated vortex motion across the full width of the cluster occurs, yielding a finite voltage. The potential for $f=\frac{3}{4}$ is identical since, as noted above, an antivortex in a cluster at flux $(1-f)$ is equivalent to the single vortex state at flux $f$. The voltages at $f$ and $(1-f)$ are also equal, since vortices driven across the array by the current-induced Lorentz force encounter the same potential as antivortices that are driven by the current in the opposite direction. In contrast, the cell minima and edge barriers in the disordered cluster are skewed. As a result, vortex motion in opposite directions is different, yielding polarity-dependent critical currents and voltages, as we observe. This accounts for the different voltages and critical currents for the $f$ and $(1-f)$ states. However, for negative bias current, an antivortex encounters the same potential as a vortex for positive current, resulting in the observed inversion symmetry through the point $(I=0, f=\frac{1}{2})$. These arguments apply equally well to larger clusters. However, when there is more than one vortex in a cluster, it is not possible to describe the dynamics by considering the motion of discrete vortices in a static two-dimensional potential. Vortices in small arrays are strongly interacting and the collective, coherent motion of the vortex distribution must be considered.

In summary, we have compared measurements and simulations of the vortex dynamics of $2\times2$ cluster arrays. Disorder in the coupling between islands that averages out in large arrays is found to have a profound effect on the transport properties of small clusters. Symmetries in the voltage versus flux response with respect to bias current and applied flux have been identified and explained within a dynamical vortex model. Modeling of cluster data enables a quantitative determination of the distribution of junction critical currents in our arrays.

This work was supported by the National Science Foundation through Grant No. NSF-DMR91-15411. We also acknowledge extensive use of the Microfabrication Facility of the Frederick Seitz Materials Research Laboratory at the University of Illinois.

[1]For a review of this field, see *Proceedings of the NATO Workshop on Phase Coherence in Superconductor Networks,* edited by J. E. Mooij and G. Schon [Physica B **152** (1988)].

[2]E. Granato and J. M. Kosterlitz, Phys. Rev. B **33**, 6533 (1986); M. G. Forrester, H.-J. Lee, M. Tinkham, and C. J. Lobb, *ibid.* **37**, 5966 (1988).

[3]W. Xia and P. L. Leath, Phys. Rev. Lett. **63**, 1428 (1989); M. B. Cohn, M. S. Rzchowski, S. P. Benz, and C. J. Lobb, Phys. Rev. B **43**, 12 823 (1991).

[4]Y.-H. Li and S. Teitel, Phys. Rev. Lett. **67**, 2894 (1991); D. C. Harris, S. T. Herbert, D. C. Stroud, and J. C. Garland, *ibid.* **67**, 3606 (1991).

[5]S. V. Rao and D. J. Van Harlingen (unpublished).

[6]P. G. de Gennes, *Superconductivity of Metals and Alloys* (Addison-Wesley, Palo Alto, 1989).

[7]M. S. Rzchowski, S. P. Benz, M. Tinkham, and C. J. Lobb, Phys. Rev. B **42**, 2041 (1990).

[8]H. S. J. van der Zant, H. A. Rijken, and J. E. Mooij, J. Low Temp. Phys. **79**, 289 (1990).